

A PARAMETRIC SHELL ANALYSIS OF THE SHUTTLE 51-L SRB AFT FIELD JOINT

Randall C. Davis
Lynn M. Bowman
Robert M. Hughes IV
Brian J. Jackson

October 1990

(NASA-TM-102748) A PARAMETRIC SHELL
ANALYSIS OF THE SHUTTLE 51-L SRB AFT FIELD
JOINT (NASA) 19 p CSCL 20K

NO1-14627

Unclass

63/39 0317629



National Aeronautics and
Space Administration

Langley Research Center
Hampton, Virginia 23665

A PARAMETRIC SHELL ANALYSIS OF THE SHUTTLE SRB AFT FIELD JOINT

SUMMARY

Following the Shuttle 51-L accident, an investigation was conducted to determine the cause of the failure. Investigators at the Langley Research Center focused attention on the structural behavior of the field joints with O-ring seals in the steel solid rocket booster (SRB) cases. The shell-of-revolution computer program BOSOR4 was used to model the aft field joint of the solid rocket booster case. The shell model consisted of the SRB wall and joint geometry present during the Shuttle 51-L flight. A parametric study of the joint was performed on the geometry, including joint clearances, contact between the joint components, and on the loads, induced and applied. In addition combinations of geometry and loads were evaluated. The analytical results from the parametric study showed that contact between the joint components was a primary contributor to allowing hot gases to blow by the O-rings. Based upon understanding the original joint behavior, various proposed joint modifications are shown and analyzed in order to provide additional insight and information. Finally, experimental results from a hydro-static pressurization of a test rocket booster case to study joint motion are presented and verified analytically.

INTRODUCTION

To assist in the investigation of the Shuttle 51-L accident, the structural analysts of the Langley Solid Rocket Motor Improved Field Joint Assessment Team focused attention on the field joints in the solid rocket booster (SRB) cases. Their objective was to determine how structural deformations in the field joint influence the elastomeric O-rings and their ability to seal the SRB field joints.

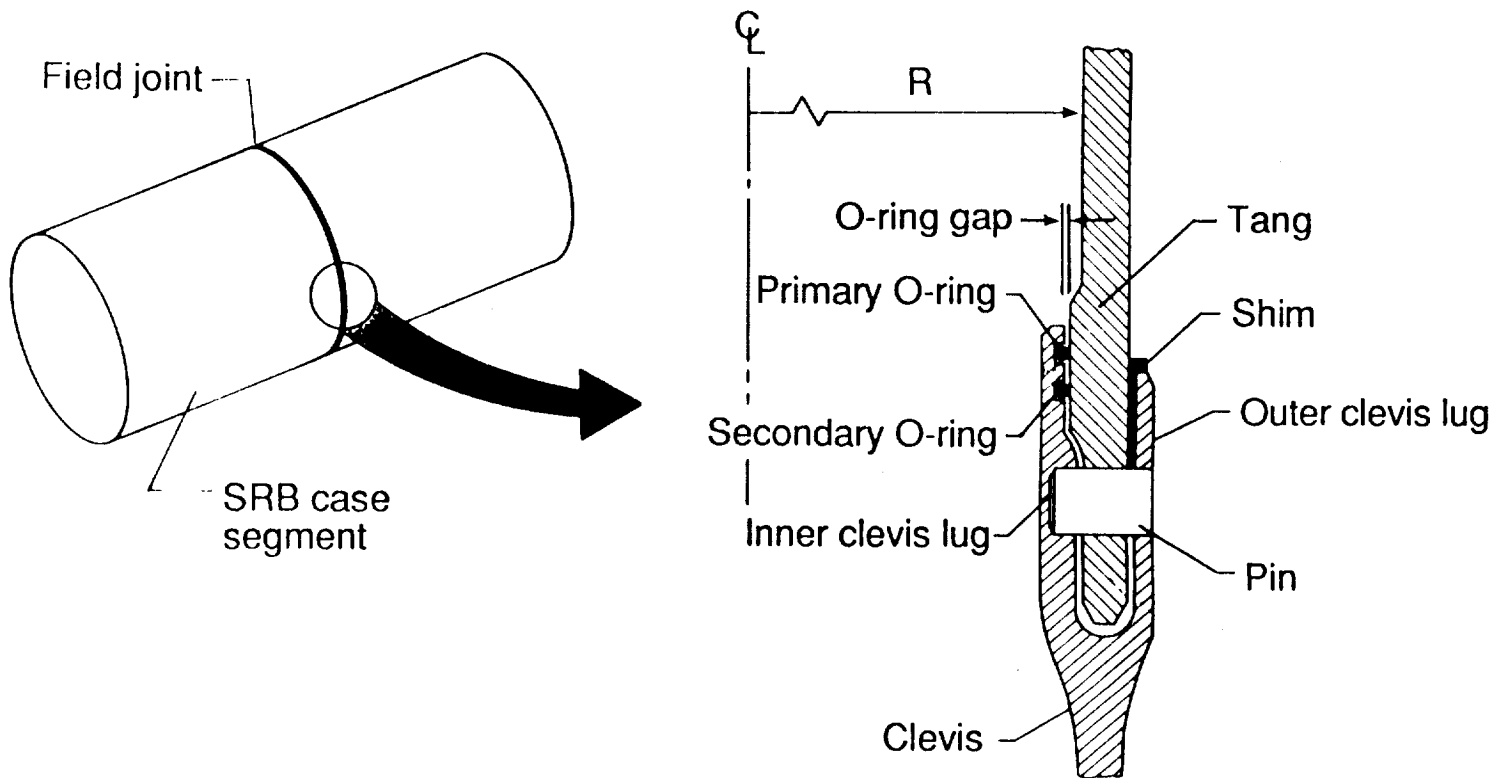
As shown in the figure, the SRB case is a segmented, thin-walled cylindrical shell. The joint between these segmented shells are called field joints due to the fact that they are assembled at the launch site. Each shell segment has two different ends; one end of a shell segment, called the tang, fits inside an annular cavity, called the clevis, on the mating shell segment. Matching holes in the tang and clevis were fitted with pins to hold the joint together. Shims were used as needed to center the tang and the clevis. The joint was sealed using two circumferential elastomeric O-rings, placed between the mating surfaces of the tang and clevis segments.

Pressurization of the SRB cases by rocket ignition during the launch sequence causes different structural deflections in the tang and clevis. This differing behavior of the tang and clevis influences the sealing capability of the O-rings and can widen the nominal gap between the tang and clevis. The nominal gap is shown in the figure as the O-ring gap.

Many structural analyses of the joint, prior to and after the 51-L accident, were performed. These analyses were predominantly of the finite element type and included many details of the joint geometry and several applied loadings. However, depending on the modeling techniques and assumptions used by the analysts, the results varied from one analysis to another. To resolve variations in computed results, a parametric study was developed to identify which structural and load parameters influenced the change in the nominal gap. The gap change throughout this study is consistently defined as the change in clearance, from the unloaded to the loaded state, between the inner clevis lug and the tang midway between the two O-ring seals.

Therefore, the objective of this parametric study is to gain an understanding of the structural mechanics of the solid rocket booster field joint and to bracket the uncertainties caused by modeling assumptions. In addition, the information obtained from this study would be incorporated into a detailed finite element model for future evaluations.

INTRODUCTION



SCOPE OF SHELL ANALYSIS STUDY

In order to accomplish the task of producing parametric results in a timely manner, a finite difference analysis program using axisymmetric shell theory, called BOSOR4 (ref. 1) was used. Several finite difference models were generated to evaluate the effects of various structural geometry and load cases. The effect of geometric nonlinearity due to the high internal pressure and axial loads experienced by the booster at lift off and the effect of the presence of the external tank stubs located near the aft field joint are presented. The non-contact behavior of the tang and clevis are evaluated to gain insight on the displacement and rotation of the joint components separately. Next the contact-interaction and clearances of the field joint are analyzed to show their effect on the O-ring gap. The field joint load cases consisted of varying the pressure distribution across the joint due to the primary and/or secondary O-ring sealing properly and varying the pin induced moments caused by the eccentric load path on the outer lug of the clevis. Based upon the results from the separate structural and load parameter variations, combinations of tang and clevis clearances and pin induced moments are analyzed to show their total effect on causing the O-ring gap to widen.

While this study was in progress, alternate joint designs were being proposed and needed rapid structural evaluation. These designs were modeled and analyzed in BOSOR4 and are presented in this study. The following is a list of designs that were evaluated: 1) Bolted Joint 2) Modified Pin joint 3) Capture-tang joint and 4) Belly bands.

Finally, referee test data was available to verify the analytical results obtained previously in the parametric study. The experimental data was useful in correlating the predicted gap openings due to the combination of the pin induced moment and tang tip clearances. The effect of pin friction on the outer lug clevis clearance and joint rotation was identified. Tang pullout and joint strains predicted by the analytical models were verified with the test data also.

SCOPE OF SHELL ANALYSIS STUDY

- Field joint structural parameters
 - effect of geometric nonlinearities
 - effect of external tank stubs
 - non-contact joint behavior
 - contact-interaction joint behavior
 - joint clearances
- Field joint loads
 - variation of pressure distribution across joint
 - variation of pin induced moment on clevis inner lug
- Combinations of structural parameters and load cases
- Evaluation of proposed designs
 - bolted joint
 - modified pin joint
 - capture-tang joint
 - belly bands
- Referee test and analysis correlation
 - gap opening due to moment and clearance
 - effect of pin friction
 - tang pullout
 - joint strains

FIELD JOINT STRUCTURAL PARAMETERS

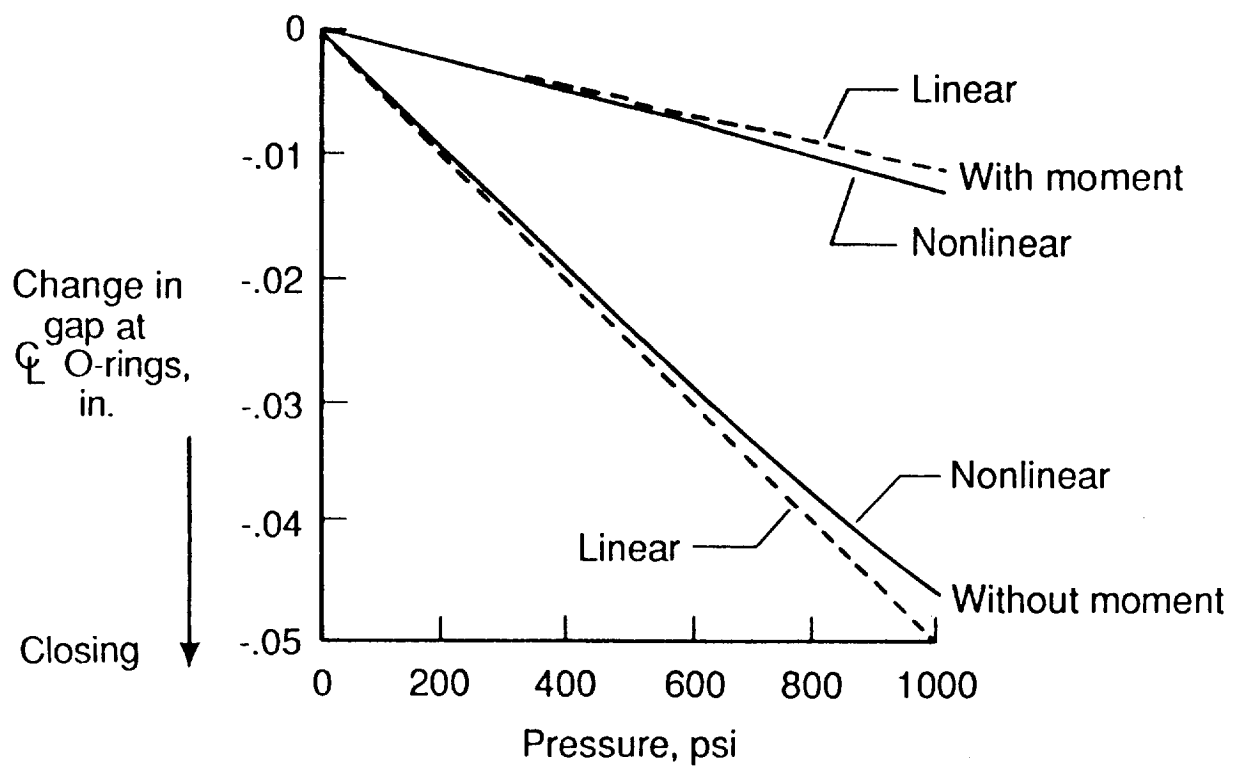
Effect of Geometric Non-linearities

A non-linear analysis was performed to assess the geometric non-linearity of the displacements due to pressure and axial load. The non-linear prestress option in BOSOR4 was used for this task. Any geometric non-linearity caused by contact or friction was ignored, and only the non-linearity due to load and large displacement was considered. The pin reactions were treated as an axial line load applied to the inner lug. For this study the pin reaction offset at the clevis inner lug was varied. All loads were increased from zero to maximum load in ten incremental steps. The change in O-ring gap is defined as the change in the clearance, from the unloaded state to the loaded state, between the inner clevis lug and the tang midway between the two O-ring seals.

In the absence of clevis/tang contact and no pin reaction offset (no pin induced moment), the O-ring gap closes. This is shown in the figure as a negative gap change to signify closure of the O-ring gap. Without a pin offset, or no pin induced moment, the gap closes by about 0.050 inch. By including the pin reaction load offset, which causes a pin induced moment, the amount of gap closure is reduced to about 0.012 inch. These plotted results show that the effect of non-linearity in the geometric shell model deformations is not as significant as the proper evaluation of the pin load induced moment. Hence, only linear stress analyses were considered in the remainder of this study. Therefore, any non-linearity associated with clevis-tang contact can be treated by using influence coefficients and linearly applied contact/reaction line loads.

FIELD JOINT STRUCTURAL PARAMETERS

Effect of geometric non-linearities



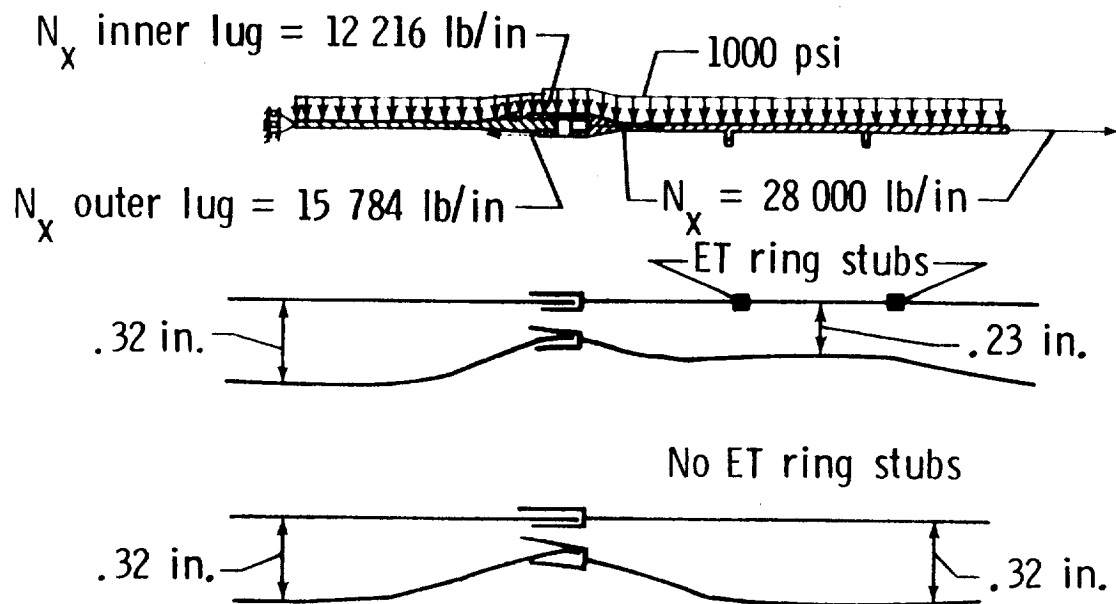
FIELD JOINT STRUCTURAL PARAMETERS

Effect of External Tank Attachment Rings

The aft field joint in the SRB case differs from the other field joints in that it is in the proximity of the attachment point for the external tank. The SRB case provides two ring stubs for attaching the external tank. These stubs require a greater shell wall thickness than the rest of the SRB case between joints. The increased stiffness due to the ring stubs and the thicker shell wall to the aft field joint was added to the separate joint models. This study analyzed the change in joint deformations due to the presence of external tank attachment ring stubs and the greater shell wall thickness adjacent to the aft field joint. The results (see figure) indicate that the proximity of these ring stubs and the thicker shell wall to the aft field joint have only a slight effect on the joint rotations and deformations. Although the radial deformations near the clevis side of the joint are reduced, the relative rotation of the tang and clevis is not greatly affected. Hence, the computed results show a reduction in the O-ring gap opening on the order of 0.005 inch as a result of stiffening of the shell wall near the aft joint for the external tank attachment. Therefore the external tank attachment details will not be included in the remainder of this study.

FIELD JOINT STRUCTURAL PARAMETERS

Effect of external tank attachment rings



NON-CONTACT JOINT BEHAVIOR Separate Tang and Clevis Models

The first objective of this study was to determine the individual behavior of the tang and the clevis. The clevis and tang sides of the solid rocket booster field joint were modeled and analyzed separately. The BOSOR4 program branched shell capability was used to model the inner and outer lugs of the clevis as shown by the branched heavy solid lines in the schematic of the clevis in the figure. BOSOR4 is limited to axisymmetric geometry, hence, the pin reactions on the tang and clevis were treated as line loads acting on the separate shell models. The tang model consisted of an 82 inch long portion of the SRB case and the clevis model consisted of an 82 inch long portion of the SRB case with a branched shell representation of the inner and outer lugs. These model lengths were arbitrary but were long enough for joint effects to decay before reaching the truncated ends of the models.

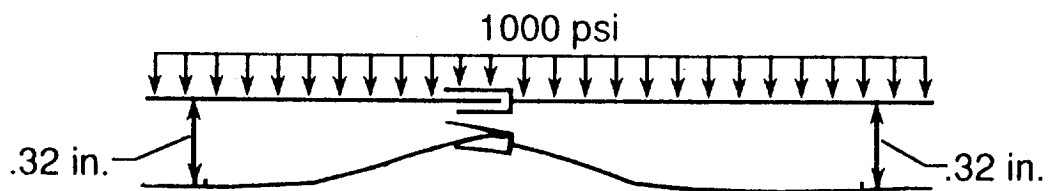
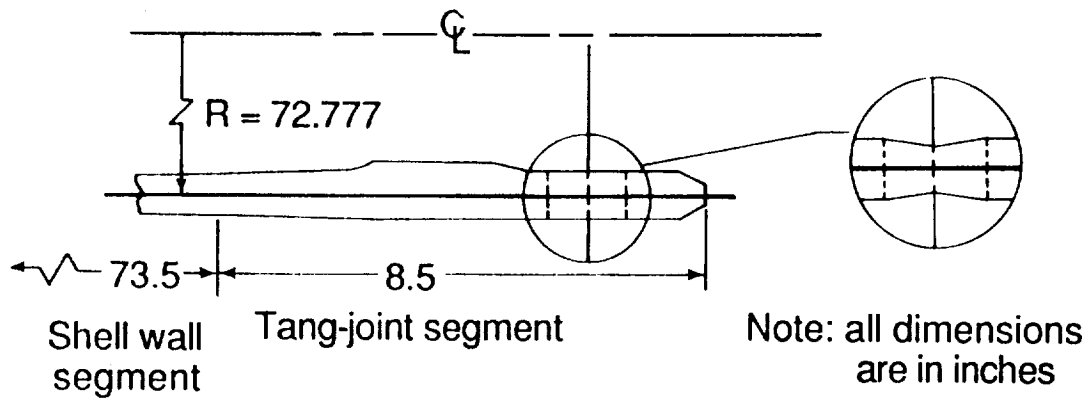
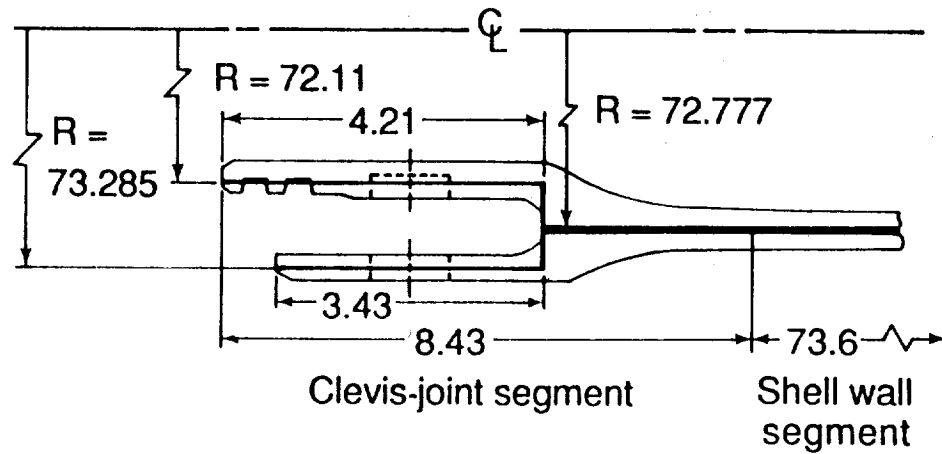
Modeling of the pin hole region in an axisymmetric shell model required special consideration. The axisymmetric shell model wall thickness was reduced across the pin hole region to an equivalent value at the center of the pin hole (see inset). To determine the reduced thickness value, while keeping the model simple for this analysis, either hoop stiffness or bending stiffness at the pin hole centerline could be duplicated but not both simultaneously. A separate study determined that the loss of axial bending stiffness due to the pin holes was more important for inner clevis lug deflections than the loss in hoop stiffness. Therefore, the reduced thickness used at the center of the pin hole was chosen to duplicate the meridional bending stiffness for the shell geometry along the centerline of the pin holes. As a consequence it was noted for later use that the corresponding hoop stiffness in the tang model was slightly greater than the actual hoop stiffness of the tang with pin holes.

For boundary conditions, the axial and circumferential displacements were constrained (zero) at the ends of the separate models away from the joint but the radial displacement was not constrained. An internal pressure of 1000 psi and an axial load of 28000 lb/in that occur at rocket motor ignition was applied to each model. The locally concentrated pin reaction loads were replaced by axisymmetric line loads acting on the shell models. The axial line load was proportioned into two line loads based on static equilibrium and applied to the clevis inner and outer lugs. The pin holes do not penetrate the inner lug, thus the center of the pin bearing surface was offset from the inner lug mid surface. Therefore, the axial line load on the inner lug was offset from the inner lug neutral axis a distance equal to this offset. Finally, the pressure loading was applied only up to the sealed side of the first O-ring groove.

The results from the analysis of the separate models of the tang and clevis indicate that the shell wall has less hoop stiffness than the joint. Thus, the shell wall displaces radially outward more than the joint when acted on by the internal pressure. As a result, the tang and clevis rotate in opposite directions relative to each other, with the tang rotating nearly twice as much as the clevis. The influence of the joint on the rocket motor case radial deflection becomes negligibly small beyond 20 inches from the pin centerline. Finally, the offset axial pin reaction load on the inner lug produces a substantial local bending moment that has a pronounced effect on the deflection of the tip of the inner lug at the O-rings.

NON-CONTACT JOINT BEHAVIOR

Separate tang and clevis models



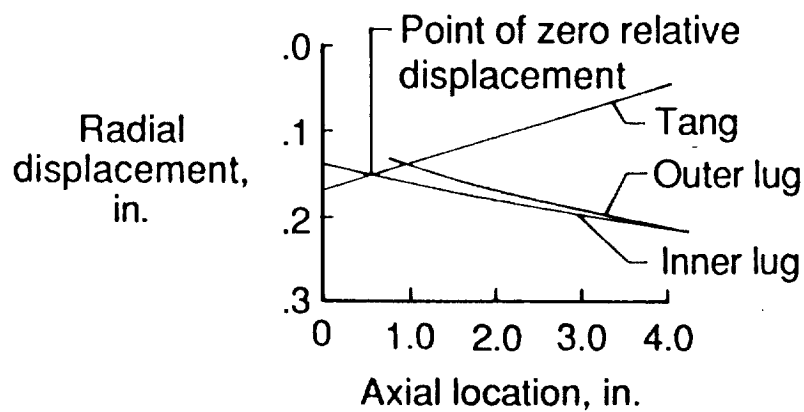
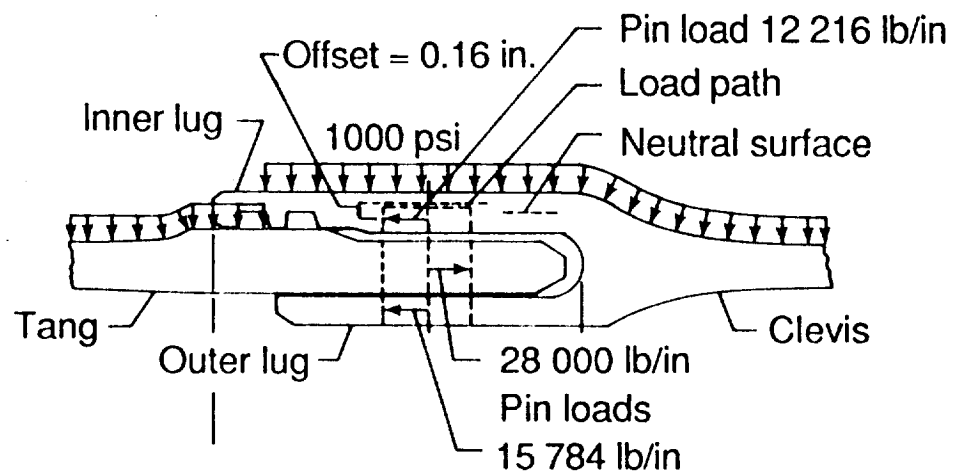
NON-CONTACT JOINT BEHAVIOR Superimposed Radial Displacements

Typical radial displacements within the joint region from the separate tang and clevis models were superimposed for ease of comparison in the figure. Using the centerline at the pins as a common axial location point between the tang and clevis, the displacements were shown plotted at their corresponding axial locations directly below the shell model. Key deductions made from an analysis of superimposed radial displacements from several runs of the two models were as follows:

- o The O-ring area of the joint moves radially outward about 0.15 inch during pressurization.
- o The tang rotates 1.8 degrees, and the clevis inner lug rotates 1.1 degrees, for a total relative rotation of 2.9 degrees.
- o Contact between the tang and clevis will occur if the outer lug tip clearance is less than 0.017 inch and the tang tip clearance is less than 0.17 inch.
- o The pressure distributed along the inner lug closes the space between the clevis lugs by about 0.025 inch at the O-rings.
- o A 0.16 inch offset pin reaction line load on the inner lug produces a substantial local bending moment that opens the O-ring gap.
- o At the pin centerline the clevis radial displacement is almost twice the tang radial displacement hence, the tang must slide along the pins or be restrained by friction.
- o There is a point of zero relative radial displacement between the tang and the clevis inner lug. As shown in the figure, this point lies very near the midpoint between the two O-rings.
- o The rotation of the tang and clevis, assuming no contact and no friction, will not open the gap appreciably.

An inspection of the engineering drawing dimensions for the joint reveals limited room for the tang to rotate inside the clevis. The drawings show a 0.01 inch nominal radial clearance at the outer lug tip and a 0.10 inch nominal radial clearance at the tang tip. Using the 0.01 inch nominal radial clearance at the outer lug tip and the 0.10 inch nominal radial clearance at the tang tip, a relative rotation of only 1.5 degrees is possible before contact takes place between the tang and clevis. The 2.9 degree relative rotation found in the analysis is greater than this and means contact will take place and the resulting interaction loads will pry open the clevis at the O-rings. Thus, contact between the tang and clevis and the resulting interaction loads are considered from this analysis to be the primary cause for the gap to open.

NON-CONTACT JOINT BEHAVIOR Superimposed radial displacements



CONTACT-INTERACTION JOINT BEHAVIOR

Outer Lug and Tang Contact

The joint design had nominal clearances between the tang and the clevis lugs. Pressurization of the rocket motor case at ignition causes the tang and clevis to displace and rotate relative to each other within the joint. As the previous results have shown these displacements and rotations can exceed the nominal clearances allowing the tang and clevis to make contact with each other. Based on the previous shell analysis results, the displacements exceeded the clearances in the joint at the outer lug tip and at the tang tip at the locations shown in the figure. Drawings show the nominal clearance at the tip of the outer lug ranges from 0.037 to 0.049 inch. During assembly of the field joint, shims nominally 0.034 inch thick were placed between the outer lug tip and the tang to eliminate 0.034 inch of this clearance, leaving a residual clearance ranging from 0.003 to 0.015 inch. This range of clearances at the outer lug tip was assessed analytically. The tang tip clearance will be considered later.

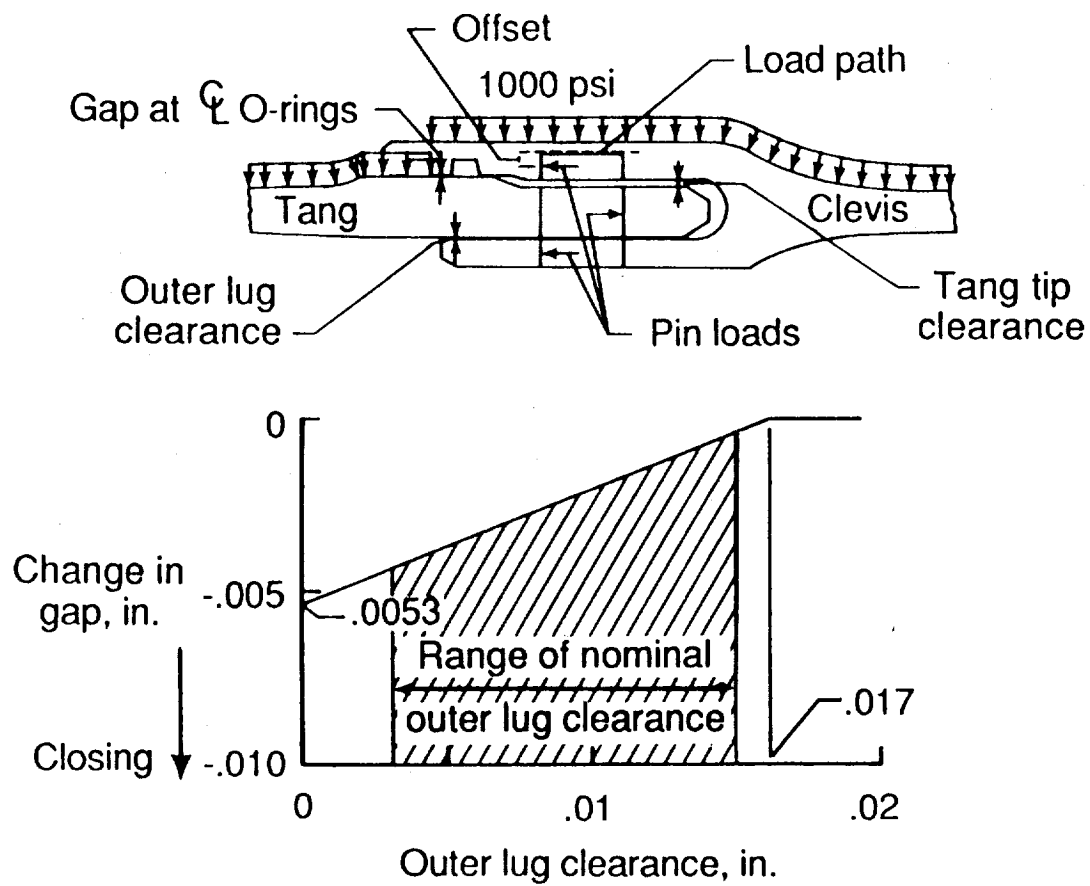
The previously shown radial displacement results indicated that the outer lug tip did not move as far radially as the adjacent point on the tang. Hence, pressurization caused the outer lug tip to contact the tang after the initial clearance was exceeded. By using influence coefficients, equal and opposite radial loads were applied to the outer lug tip and the tang to duplicate the effect of contact between the two components. The influence coefficients were used to find radial loads that enforce relative radial displacements equal to the initial clearance. The change in the O-ring gap, relative to the no contact baseline result, is shown in the figure for varying amounts of outer lug-to-tang clearance with the SRB motor case fully pressurized. The results show that such contact tends to close the O-ring gap. As shown in the figure, for a clearance greater than 0.017 inch, no contact takes place between the outer lug and tang and the change in the gap is zero. On the other hand, if the clearance is zero, the outer lug pushes radially inward on the tang and the tang pushes radially outward on the outer lug. The result is a closure of the O-ring gap by about 0.0053 inch as shown in the figure.

Based on these results, opening of the O-ring gap will be minimized if the outer lug clearance is zero. This implies that as large a shim as possible should be placed between the outer lug and tang. Also note that the increase in O-ring gap opening is equal to about one third of the increase in clearance at the outer lug tip.

The results shown are based on a model with the outer lug pin reaction load passing through the neutral axis of the outer lug. If the outer lug pin reaction is offset slightly (due to mismatch or deformations, etc.), a moment is induced in the outer lug. Including this moment in separate analyses shows that an offset to the tang side of the outer lug neutral axis causes a deflection of the lug tip away from the tang, which adversely affects the O-ring gap.

CONTACT-INTERACTION JOINT BEHAVIOR

Outer lug and tang contact



JOINT CLEARANCES

Tang tip and Clevis Contact

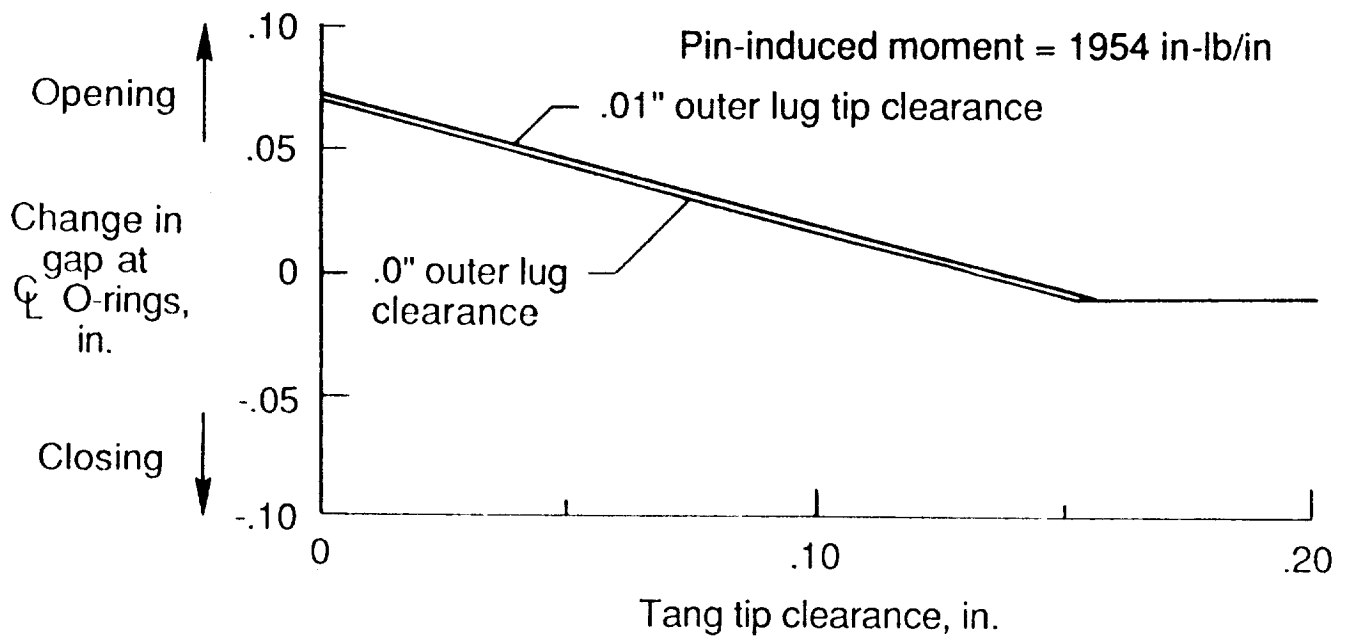
As the previous results have shown, contact between the outer lug tip and the tang will occur for the range of nominal outer lug tip clearances that are available. Contact between the outer lug tip and tang produces radial loads that push the tang radially inward and the clevis and radially outward. These forces will cause contact between the tang tip and the clevis inner lug. All of these radial contact loads were determined by using a force/stiffness technique. A basic load case was first analyzed with the model under pressure with no contact. The radial clearances at the tip of the outer lug and at the tip of the tang were subtracted from the displacements in these two areas. These difference values between the displacements and clearances were used with unit radial loads separately applied at these locations to compute load-deflection or influence coefficients. Using the influence coefficients and treating the displacement-to-clearance differences as unknowns, radial loads were computed by matrix inversion that produce displacements in the model that differ by an amount equal to the prescribed clearances. The computed radial contact loads were applied to the tang and clevis models along with the pressurization loads. By the influence coefficient technique, a range of prescribed clearances was analyzed to produce the results shown graphically in the figure.

As the results in the figure indicate, the overall effect of tang tip and clevis inner lug contact is to open the O-ring gap. The plot shows O-ring gap opening (or closing) for a varying amount of tang tip clearance at two fixed values of outer lug clearance. The shell analysis results show that with sufficient clearance at the tip of the tang (greater than about 0.17 inch), the O-ring gap closes during pressurization of the rocket motor case. This contact between the tang and the clevis, brought about by their relative rotations, is the single largest cause for the O-ring gap to open.

Based on these results and the results from the previous figure, the effect of the O-ring gap opening will be minimized if the clearance at the tang tip is made larger than 0.17 inch and the clearance at the outer lug is reduced to zero with shims.

JOINT CLEARANCES

Tang tip and clevis contact



FIELD JOINT LOADS

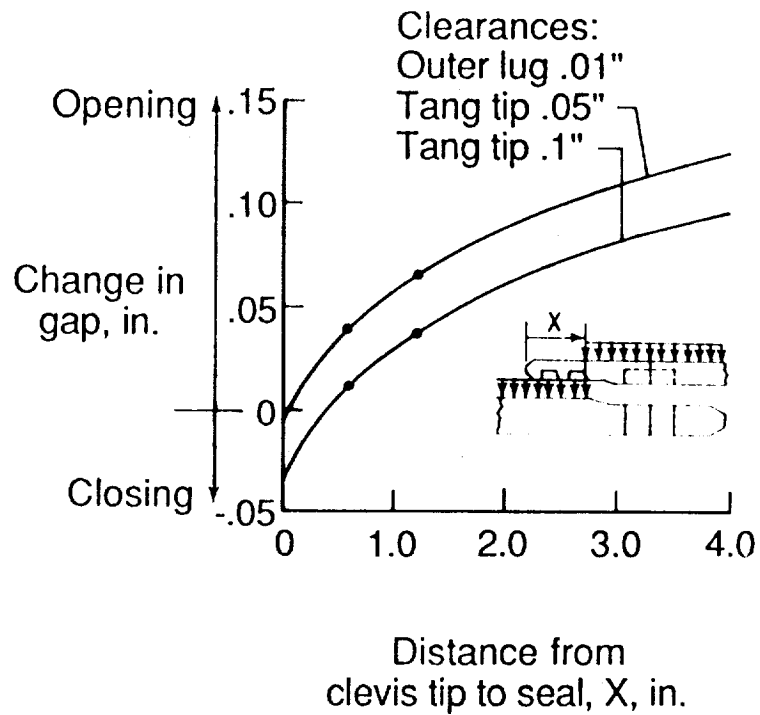
Variation of Inner Lug Pressure Distribution

The internal pressure on the SRB case across the joint was applied to the inner lug of the clevis. In particular, this pressure on the inner lug began at the centerline of the O-ring seal and extended across the joint along the clevis. Likewise the pressure on the tang started at the O-ring seal and continued along the tang and shell wall. Should the first O-ring not seal, this beginning point would shift along the tang and clevis to the second O-ring. If the annular opening at the tip of the clevis inner lug became plugged, the beginning point would shift to the tip of the clevis inner tang.

This analysis assessed the affect of the following pressure distributions on the change in gap opening: (1) a joint with the pressure beginning at the tip of the clevis inner lug ($x = 0$ in the figure) and extending along the entire length of the inner clevis lug, (2) a pressure distribution beginning at the first O-ring ($x = 0.6$ in.) which is the base case for all of the other analyses, and (3) a pressure distribution simulating a first O-ring failure where the pressure begins at the second O-ring ($x = 1.2$ in.). Although these pressure distribution cases begin at discrete locations or x values in the models, the change in gap results are shown in the figure as a continuous curve to emphasize the trend in the change in gap opening due to the various pressure beginning points. The results shown in the figure include tang and clevis contact, and the resulting contact reaction loads, if the relative deflections exceeded the two tang and clevis clearance values indicated. The results for $x > 3.0$ in. indicate that any failure to seal by one or both O-rings produces a significant amount of gap opening. Thus if the O-rings do not seal on the first pulse, the escaping gases will open the gap and hinder sealing by the O-rings. The increase in gap opening due to a shift in sealing from the primary O-ring to the secondary O-ring is about 0.039 inch. The results show that this increase in gap opening is independent of the amount of tang clearance.

FIELD JOINT LOADS

Variation of inner lug pressure distribution



FIELD JOINT LOADS

Variation of Pin Induced Moment on Clevis Inner Lug

The pin holes do not penetrate all the way through the clevis inner lug. As a result, each pin produces an axial reaction load that was offset from the load path or neutral surface of the inner lug as shown in the schematic in the figure. The reaction load and its offset from the effective load path through the inner lug, produce a pin-induced bending moment on the inner lug. This pin-to-clevis load transfer is locally concentrated and the exact magnitude of the pin-induced moment, as an equivalent axisymmetric shell line moment, was difficult to assess. However, for a parameter study, a range of moments was examined to bracket the influence of such a pin induced-moment on the O-ring gap.

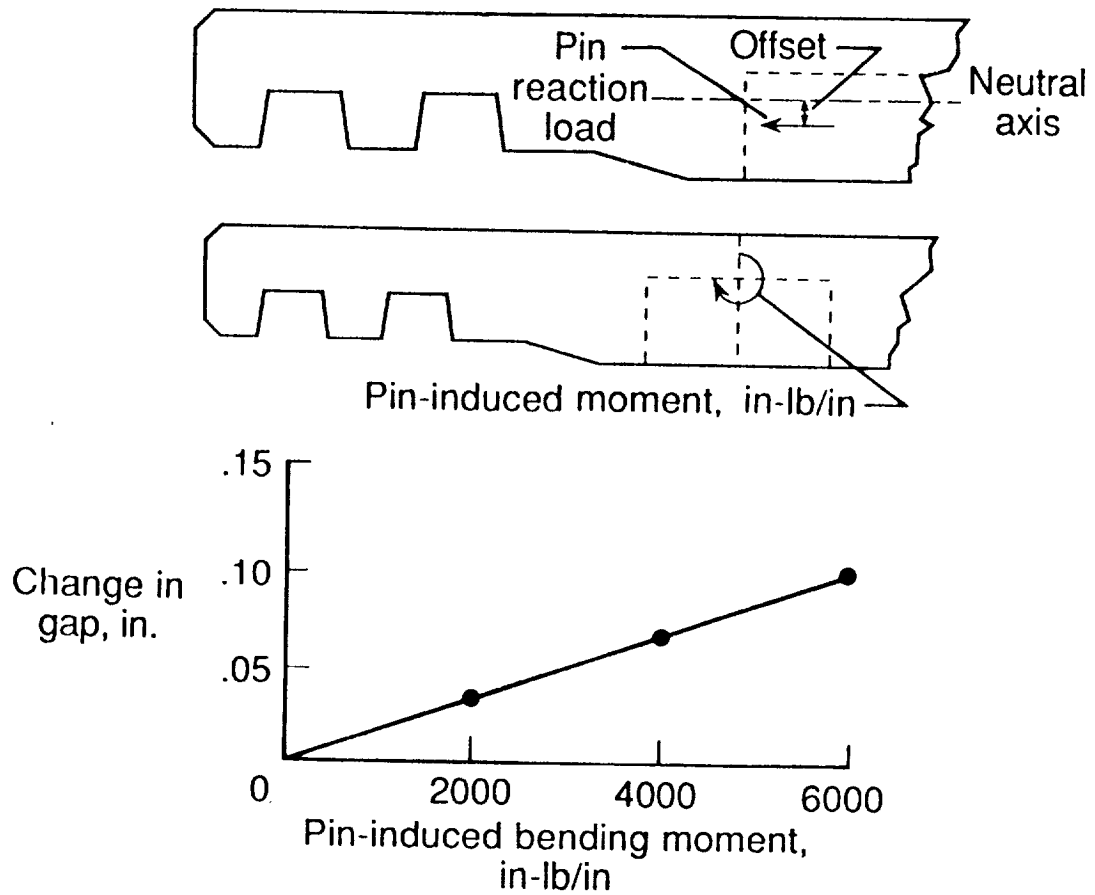
To apply a pin-induced bending moment to any shell model, there are two basic approaches. First, a line moment can be applied to the shell model or secondly, an axial load can be applied at an offset distance from the shell neutral surface. In the first approach, a zero moment analysis is made by simply setting the moment equal to zero. In the second approach, the offset must be reduced to zero while maintaining the axial load. It is noted that in the offset approach, a zero moment case cannot be correctly analyzed by setting the axial load to zero for the SRB case for the following reason. The axial load, through a Poisson effect, reduces the shell wall radial displacement caused by the pressure. Such a reduction in the shell displacement consequently alters the joint rotations and affects the gap opening. Therefore, if the offset approach is used to make a zero-moment analysis of the SRB case by setting the axial load to zero, the resulting analysis will significantly underestimate the gap opening.

Four analyses were made to show the severity of the underestimated gap opening by setting the axial load to zero in the offset approach above. An analysis with no axial load was compared with an analysis having an axial load with no offset (no pin-induced moment). The results showed a difference in closure of the gap of 0.0257 inch. Next, an analysis with no axial load was compared with an analysis having an axial load with an offset (a pin induced moment). The results showed a difference in gap closure of 0.0137 inch. These results show that a comparison procedure using an offset with and without an axial tension load (supposedly to isolate the change in gap due to a pin-induced moment) underestimates the effect of the pin-induced moment by almost a factor of two.

For the results shown in the figure, the model has an axial load with the pin-induced moment applied as a line moment. The affect of varying amounts of pin-induced moment on the gap relative to the zero moment case is shown. With no contact interactions considered, the results show that the effect of the pin-induced moment is quite large. The best estimate for the line moment load is 2000 in-lbs/in which produces a 0.033 inch increase in the gap opening. This is the result of a 0.16 inch offset and a pin reaction line load of 12,216 lbs/in on the inner lug.

FIELD JOINT LOADS

Variation of pin induced moment on clevis inner lug



COMBINATIONS OF STRUCTURAL PARAMETERS

Effect of Combined Tang and Clevis Contact on the Gap

The previous results have shown that contact between the tang and clevis generates radial loads that counter the relative rotation between the tang and clevis. The resulting radial loads tend to pry the clevis open, adversely affecting the O-ring gap.

Based on an analysis of the joint dimensions in engineering drawings, the best estimate for clearances and pin reaction offset were as follows:

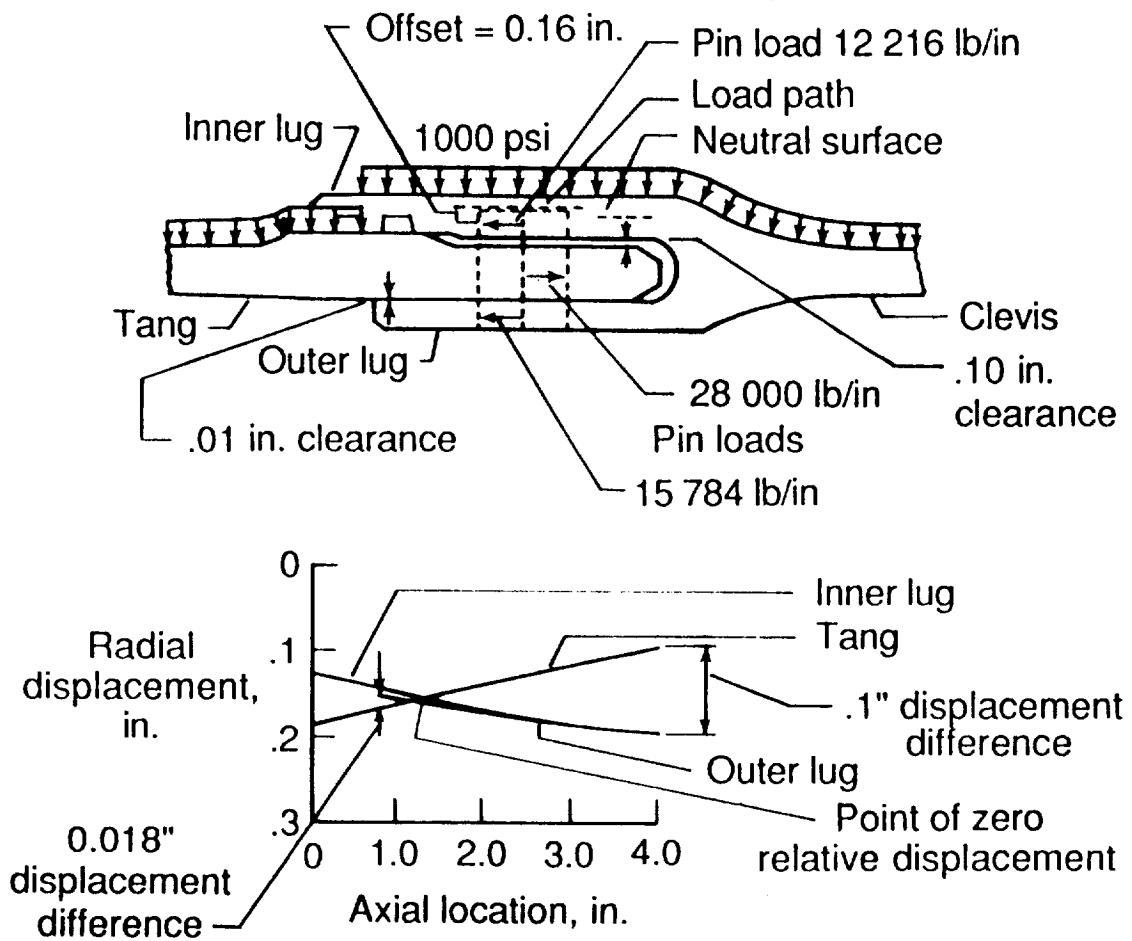
- o A 0.1 inch tang tip/clevis clearance
- o A 0.01 inch outer lug/tang clearance
- o A 0.16 inch offset for the inner clevis pin reaction.

Using these values, the influence coefficient technique described in the previous analysis was used to produce the results shown in the figure. This analysis gave a best estimate of the effect of all of the factors working simultaneously on the O-ring gap. The gap opening was found to be 0.018 inch.

The radial displacement at each longitudinal location along the tang and clevis is shown in the figure directly below the sketch the model. Compared with the earlier radial displacement results with no contact, these results show that contact between the clevis and tang nearly eliminates the 0.025 inch clevis-inner-lug-to-outer-lug closing caused by the pressure on the inner lug. Also, the point of zero relative displacement between the tang and inner clevis lug moves from a point near the O-rings to a point close to the centerline of the pins. Finally, the O-ring gap changes from a nearly closed condition to an open condition due to the contact between the tang and clevis.

COMBINATIONS OF STRUCTURAL PARAMETERS

Effect of combined tang and clevis contact on the gap



COMBINATIONS OF STRUCTURAL PARAMETERS AND LOAD CASES

An Envelope of Gap Openings

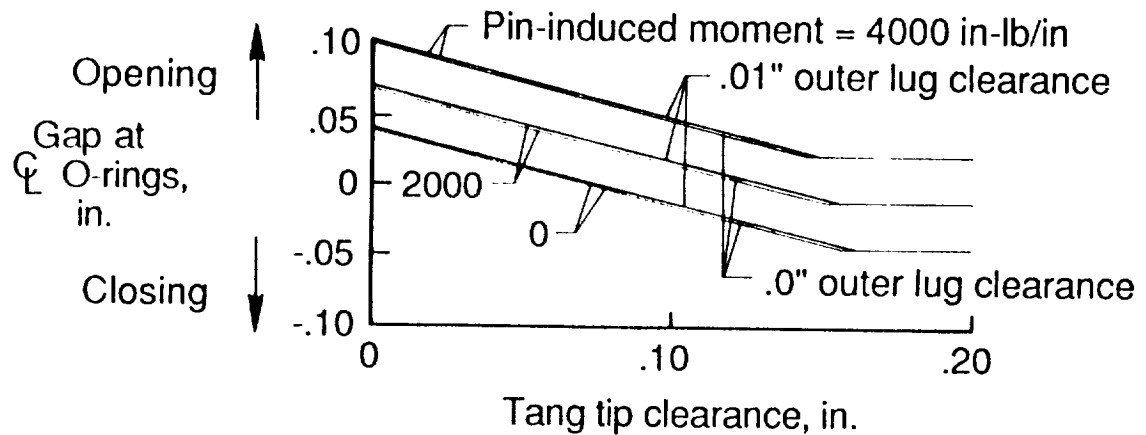
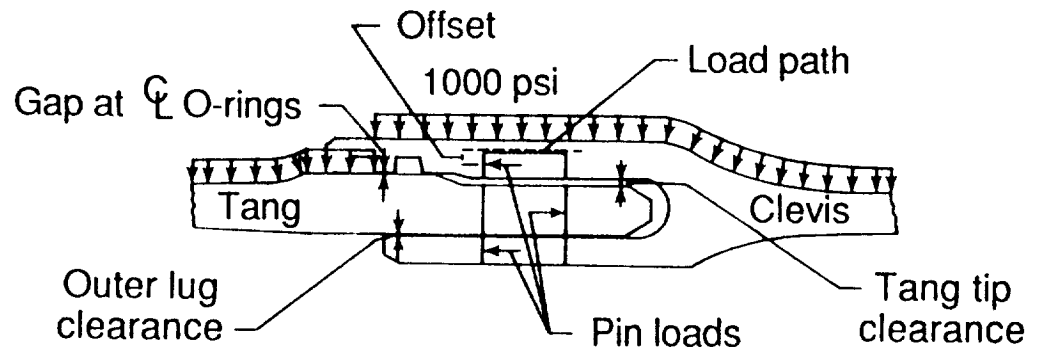
The previous results have shown that contact between the tang and clevis has a pronounced effect on the joint behavior. Based on the understanding gained from the previous analyses, a range of clearances and pin induced moments were analyzed. Their combined effect on the gap opening is shown in the figure and provide a graphical representation of the mechanics of the joint under pressurization. The clearances were numerical values enforced through influence coefficients and the pin-induced moments were applied line moment loads.

The exact amount of pin induced moment on the inner lug was difficult to assess, but the 1500 to 2000 in-lb/in axisymmetric line moment range used in previous figures was considered a good estimate. Results in previous figures have shown that the outer lug tip clearance has only a small effect on the gap and the values of 0.0 and 0.01 inch used for this figure were considered to be adequate upper and lower limits for computing gap openings.

As can be seen from the curves in the figure, eliminating the pin-induced moment and providing adequate tang-tip-to-clevis clearance would produce gap closing under pressurization. If a pin-induced moment is present, the tang-to-clevis tip clearance should be 0.14 inch or greater for the O-ring gap to close. If the pin induced moment is eliminated, the required tang tip clearance for the O-ring gap to close is reduced by one half to only 0.07 inch.

COMBINATIONS OF STRUCTURAL PARAMETERS AND LOAD CASES

An envelope of gap openings



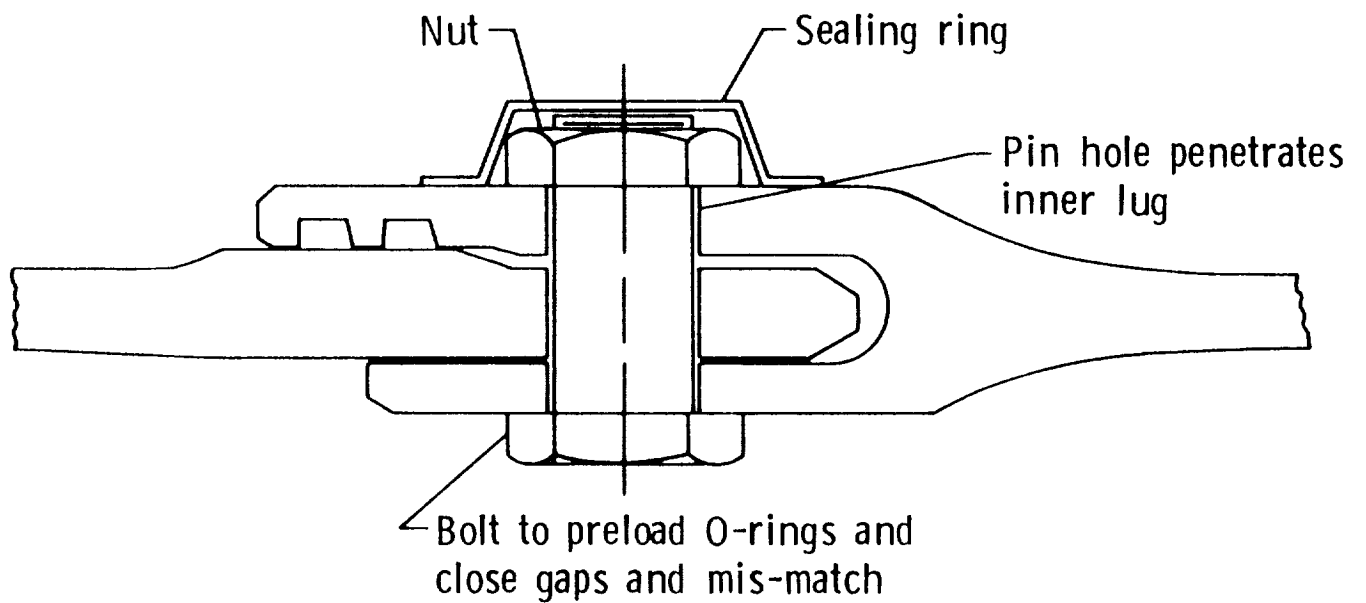
EVALUATION OF PROPOSED DESIGNS

Bolted Joint

An understanding of the joint behavior seen in the previous results, led to a joint modification that closes the O-ring gap. In the modified joint shown in the figure, the clevis geometry has a pin hole that penetrates the inner clevis lug to eliminate the pin-induced moment. Furthermore, a bolt was used instead of a pin with the bolt threaded into a captive nut or made with a twist lock on the inside of the shell wall. Preload required in the bolt is only a small fraction of the bolt strength, and only enough preload to close the gap and overcome mismatch is needed. The pin holes and nuts on the inner clevis lug were covered by a sealing ring fastened to the inside of the shell wall in any one of a number of different ways. (Soldering and brazing the sealing ring in place during heat treatment were considered to be possible methods). Analysis of this design shows that the absence of a pin-induced moment and a tang-tip clearance greater than 0.10 inch causes the O-ring gap to close under pressurization. The addition of a bolt preload of 2000 to 3000 lbs ensures that the gap remains closed during pressurization.

EVALUATION OF PROPOSED DESIGNS

Bolted joint



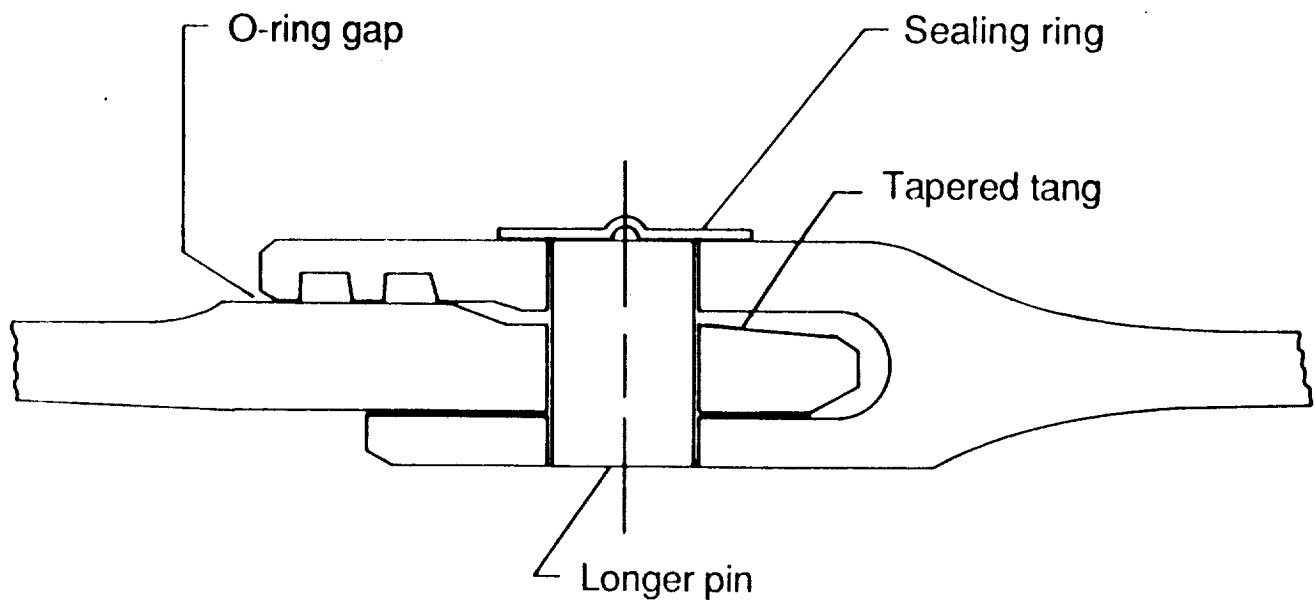
EVALUATION OF PROPOSED DESIGNS

Modified Pin Joint

Based on the previous analytical results, another modified joint concept was conceived that would provide a hydro-static proof test to verify analytical understanding of the structural mechanics of the joint. Furthermore, this modified joint would provide proof that the O-ring gap can be made to close with a simple fix to the existing design. The concept shown in the figure, used modified joint pin holes that were bored through the clevis inner lug and covered by a sealing ring adhesively bonded in place. Analysis showed that the sealing ring must have a convoluted shape (inch worm shape) to ensure that the sealing ring does not transfer axial load (thereby inducing a moment in the inner lug). Because the bore-through lengthens the pin holes, a slightly longer pin was needed. In addition, the tip of the tang was tapered slightly on the inside to ensure a clearance greater than 0.10 inch between the tang tip and the clevis. Analysis of this concept shows that the O-ring cap closes under pressurization. The proposed hydro-static pressure could be pulsated at high frequency after initial load up to relieve the friction loads on the pins, and with ample tang tip clearance, comparing results from tests with and without the pulsating pressure would assess the effect of pin friction loads on the joint behavior.

EVALUATION OF PROPOSED DESIGNS

Modified of pin joint



EVALUATION OF PROPOSED DESIGNS

Capture-Tang concept

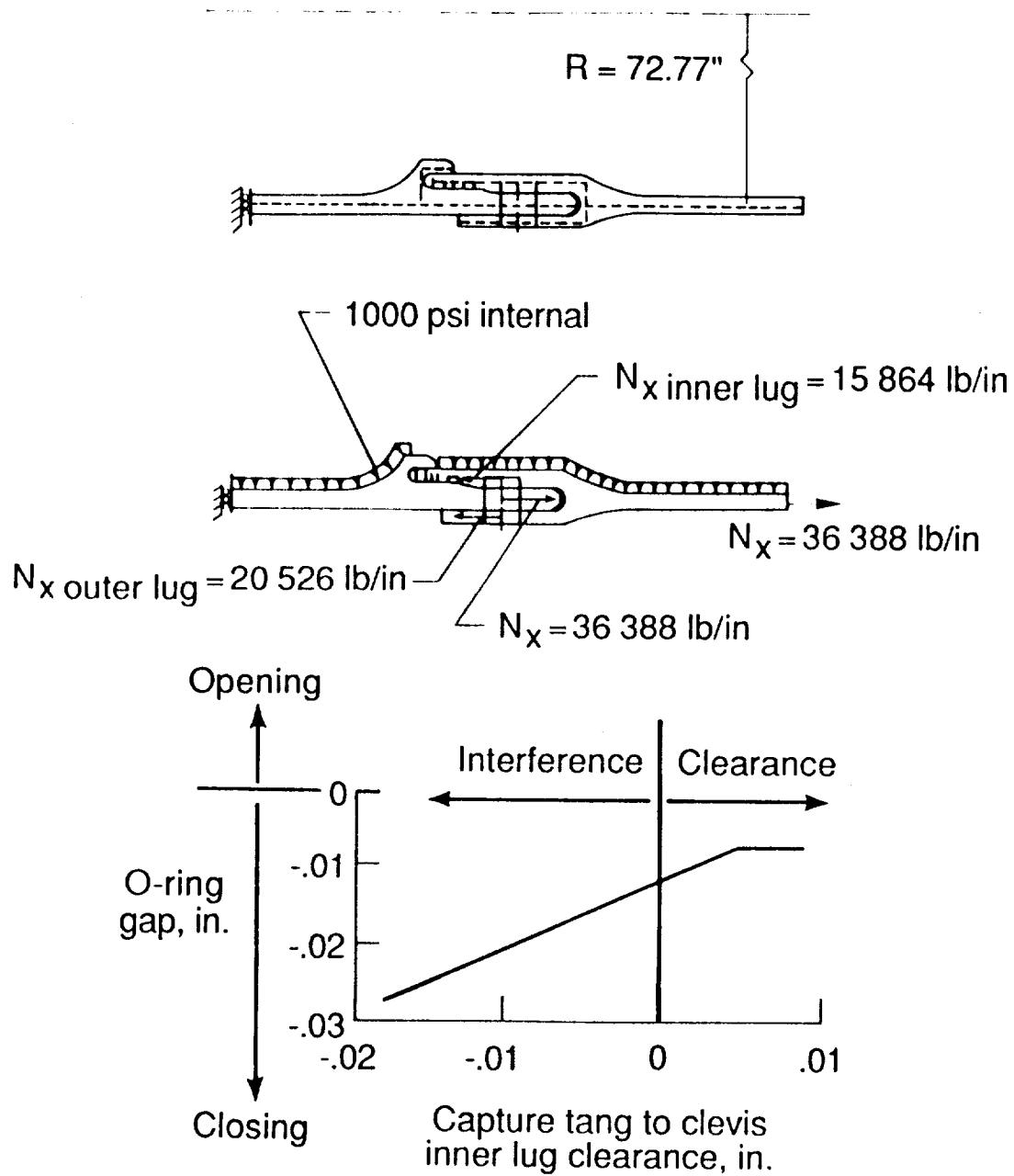
Another joint modification considered used a capture-tang to prevent the O-ring gap from opening. The capture-tang was an integral part of the tang and designed to capture the tip of the clevis inner-lug. An analysis of this modified joint showed that the material added by a 1.0 inch long by 0.40 inch thick capture tang acts as a ring added to the existing joint geometry. The presence of this additional ring material reduced the amount of tang rotation and hence reduced the relative rotation between the tang and clevis. As a result, the ring material alone was sufficient to ensure that the gap opening closes. Contact between the capture tang and the inner lug is not needed.

The capture-tang joint was assumed to have a 0.01 inch clearance at the outer lug and a 0.10 inch clearance at the tang tip. The computed change in gap for this model, without capture tang contact, is -0.007 inch (gap closes).

For a clearance between the capture tang and the outer lug greater than 0.005 inch, the capture tang does not contact the inner lug and the O-ring gap closes by -0.007 inch. For a capture tang clearance less than 0.005 inch, pressurization causes the capture tang to contact the inner lug and contact interaction loads cause the O-ring gap to close. For a capture tang clearance of zero and less (interference fit), the O-ring gap is forced to close. A 0.018 inch interference fit at the capture tang forces the O-ring gap to close by -0.027 inch.

EVALUATION OF PROPOSED DESIGNS

Capture-tang concept



EVALUATION OF PROPOSED DESIGNS

Belly Band Sizes and Locations

On the premise that relative rotation between the tang and clevis causes the O-ring gap to open, an alternative to forcing the gap to close was to stop the rotations within the joint. Rings or "belly bands" on either side of the joint were considered as a means of eliminating rotation of the tang and clevis. An analysis was made to determine the size and location for such bands to produce a zero relative rotation angle between the tang and the clevis.

A baseline band was used that had a 6 inch by 1.9 inch band of carbon fiber composite material with a modulus of 22,700,000 psi. The stiffness properties of the band were used to compute an equivalent ring for the shell model. This was done so that the ring could be attached to the shell model at a discrete location on the shell wall. The discrete location was varied along the shell length and the computed rotation results were used to find the best position for the belly band. To find the proper size band, the size of the baseline band was changed by simply changing all of the cross-sectional dimensions by the same factor and recomputing the equivalent ring stiffness properties. No interaction or contact between tang and clevis was considered in this analysis since the object was to eliminate rotations in the joint.

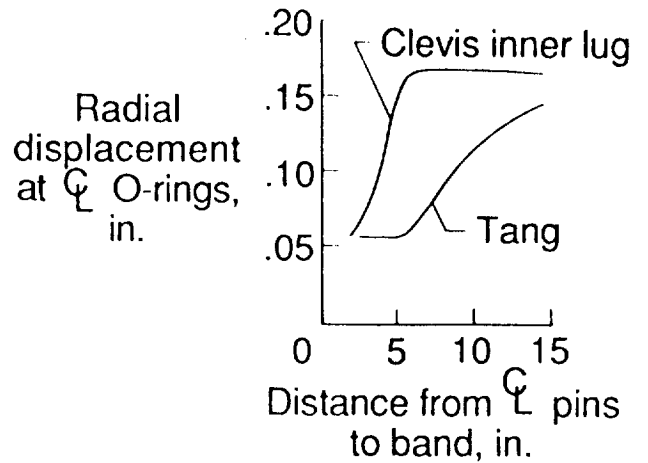
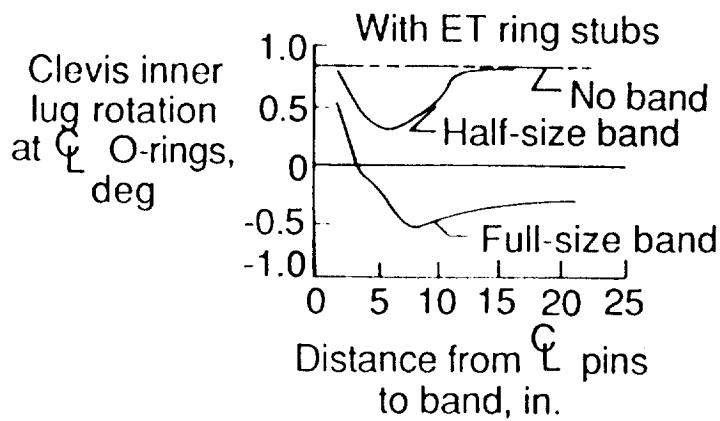
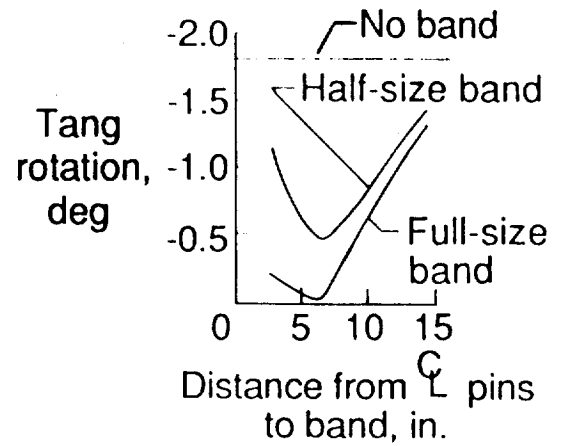
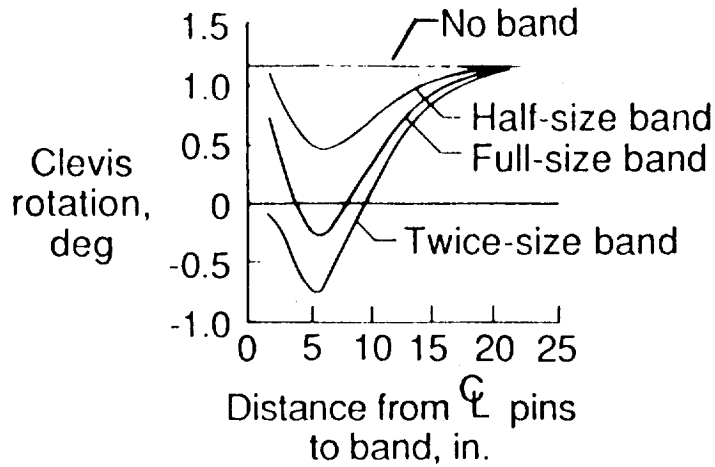
The computed tang rotation angle and the clevis inner lug rotation angle for varying band locations and sizes are shown in the figure. With no belly band the tang rotates (negative angle) in a direction opposite to the clevis (positive angle) as shown in the figure. The clevis side requires a band size 80% of the baseline and the tang side require a band 105% of the baseline for a zero rotation angle. The best position for the bands to have the most effect on the joint rotations is 6 to 7 inches from the pin centerline for both the tang and clevis.

The external tank ring stubs affect the size and location of the band needed for the clevis. A band size 68% of the baseline and located 7 inches from the pin centerline produces a zero joint rotation in the clevis if the external tank attachment ring stubs were present.

The band sizes and locations were selected on the basis of producing a zero rotation. However, as shown in the figure the resulting radial displacements of the tang and clevis are no longer equal. Achieving zero relative rotation and zero relative displacement simultaneously with just belly bands is not feasible. As the radial displacement results show, locating belly bands at 6.5 inches for both the tang and the clevis, produces a radial mismatch of about 0.10 inch at the O-rings. This large mismatch leads to contact and load interaction between the tang and clevis. Since the clevis moves further radially than the tang, this contact causes interaction forces that adversely affect the O-ring gap. Although belly bands can be used to stop rotations within the joint, they introduce a host of other difficulties that must be addressed.

EVALUATION OF PROPOSED DESIGNS

Belly band sizes and locations



EVALUATION OF PROPOSED DESIGNS

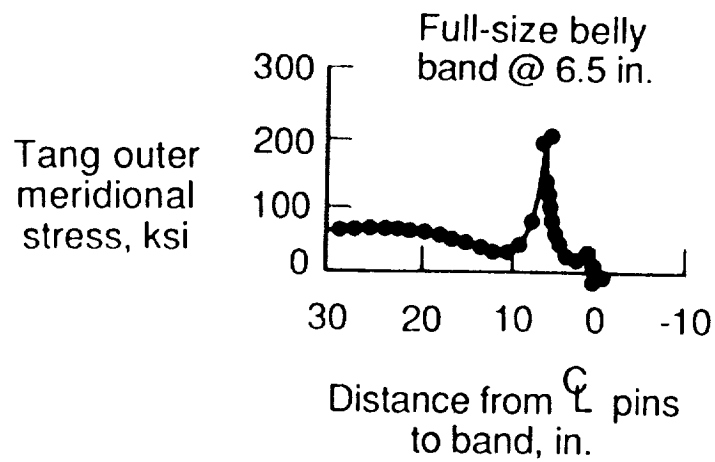
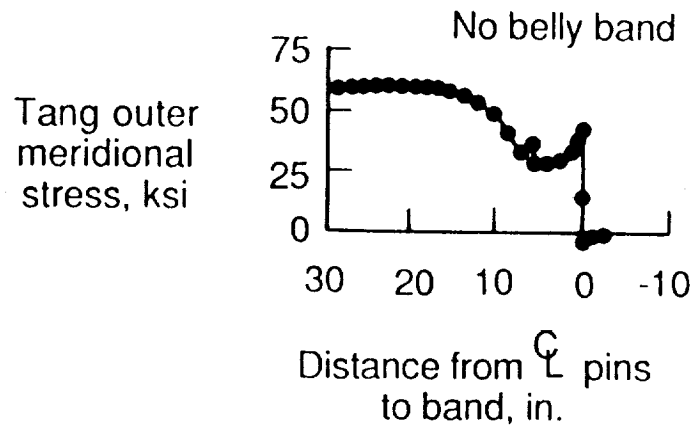
Belly Band Induced Stress

In the previous results, belly band size and location were selected on the basis of producing a zero rotation for the tang and for the clevis. The belly bands, however, also adversely affect the stresses in the rocket motor case. The first figure shows the stress distribution along the outer shell wall for the tang with no belly band. The stresses are all well below 75,000 psi.

The second figure shows shell stresses for a belly band, sized and located for zero rotation. Such a belly band creates a tang peak meridional bending stress in the shell wall outside of to the joint of the order of 200,000 psi. Therefore, an increase in the shell wall thickness is required to reduce the analytical stress. The increased shell wall thickness in turn affects the size and location of the band needed for zero rotation. This in turn affects the stresses. The end result of all of these compounding effect is a substantial increase in shell wall thickness, and hence shell weight. The increased shell weight must be added to the belly band weight to achieve zero rotation in the joint. The resulting joint design would be prohibitively heavy.

EVALUATION OF PROPOSED DESIGNS

Belly band induced stress



REFEREE TEST AND ANALYSIS CORRELATION

Gap Opening Due to Pin Induced Moment and Joint Clearances

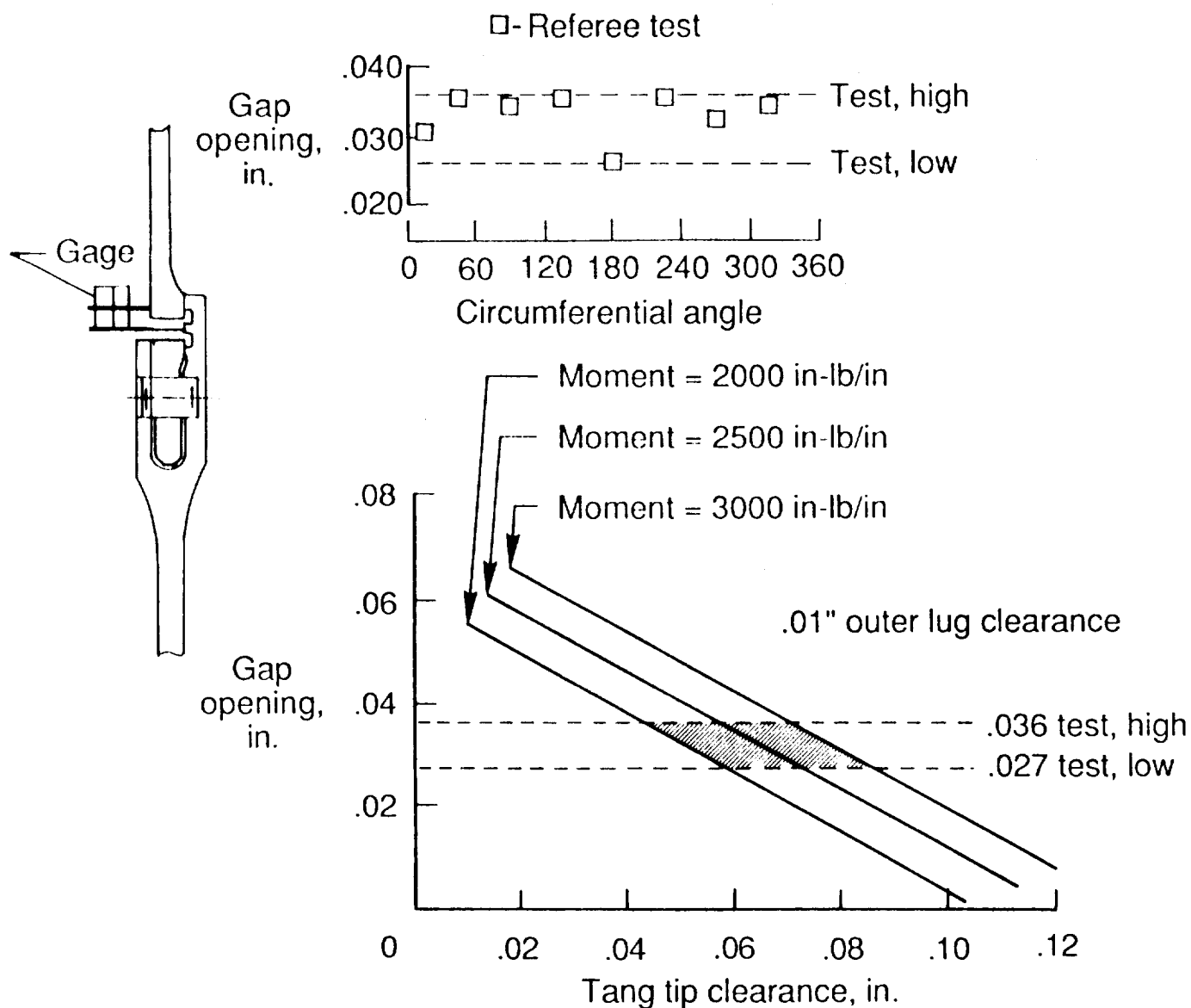
A hydrostatic pressure test of a segment of the SRB case, called a reference or a referee test (ref. 2) was conducted earlier in the shuttle program to validate analytical results. In the referee test, the tang was manufactured with ports to access the annular cavity between the O-rings, tang and clevis inner lug. Displacement gages were passed through these ports to measure the displacement of the inner lug relative to the tang. The location of these displacement gages is shown in the schematic to the left of the figure. The displacement measured by these gages is the gap opening. As shown in the figure, the gap opening measured from eight locations around the circumference of the joint ranges from a low of 0.027 inch to a high of 0.036 inch.

To compare analytical results from BOSOR4 with the hydro-static referee test, the shell model was loaded with the 1000 psi internal pressure and 36,388 lb/in axial line load induced in the test SRB motor casing. Using static equilibrium, the axial loads on the clevis were 15,876 lb/in on the inner lug and 20,512 lb/in for the outer lug. Though the actual clearances existing in the referee test are unknown, they do have the greatest influence on gap opening. But since the outer lug tip clearance has been shown to have a small effect on the gap, a single outer lug tip clearance of 0.01 inch has been used for this analysis. Therefore, joint displacements were computed for an outer lug clearance of 0.01 inch combined with pin-induced bending moments on the inner lug varying from 2000 to 3000 in-lb/in and a range of tang tip clearances ranging from 0 to 0.12 inch. Influence coefficients were used to compute radial loads at the tang tip and at the outer lug tip to produce the displacements corresponding to the specified range of tang tip clearances.

The analytical and measured gap openings are shown in the figure. The high and low range of measured gap openings are shown by the dashed lines. The analytical results represented by the solid lines are bounded by these dashed lines to produce the cross-hatch as shown in the figure. The cross-hatch brackets the gap opening associated with the 2000 in-lb/in and 3000 in-lb/in pin-induced moment and tang tip clearance that may have existed in the referee test. These results show that for an outer lug clearance of 0.01 inch in combination with a pin-induced moment from 2000 to 3000 in-lb/in, the tang tip clearance is analytically determined to be between 0.043 and 0.086 inch.

REFEREE TEST AND ANALYSIS CORRELATION

Gap opening due to pin induced moment and joint clearances



REFEREE TEST AND ANALYSIS CORRELATION

Effect of Pin Friction on Outer Lug Motion

In the referee test, displacement gages located as shown, measured the relative motion of the clevis outer lug relative to the tang during pressurization. An analysis of the joint model showed that the outer lug moves toward the tang. This analytical outer lug displacement with pressure, assuming no contact, was linear and follows the line labeled "no friction and no contact" shown in the figure. If the friction is sufficient to prevent the tang from sliding along the pins, the rate of outer lug displacement with pressure is much greater and follows the curve marked "friction, no contact" shown in the figure.

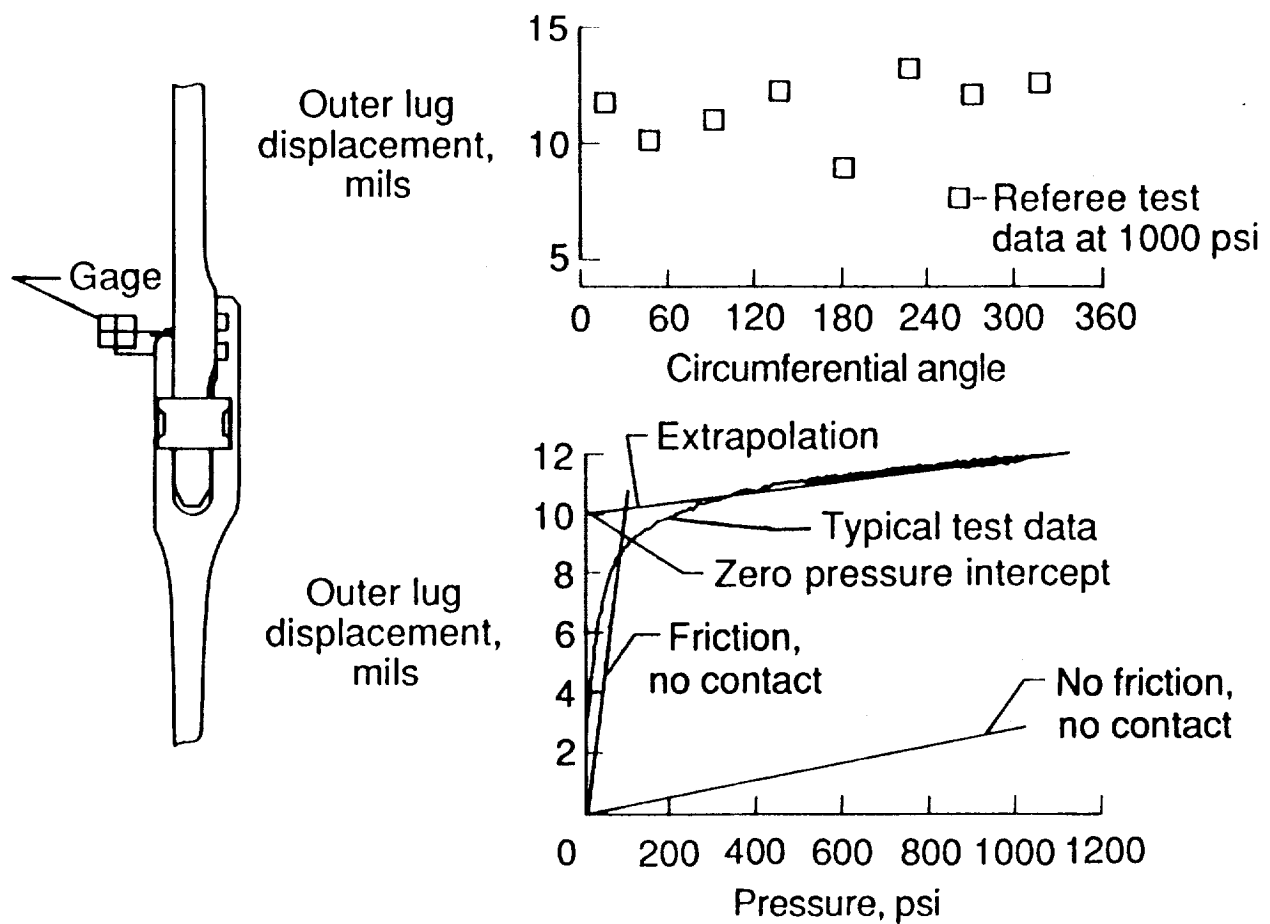
In the referee test, the axial load is transferred by the pins from tang to clevis. This axial load on the pins combines with relative radial motion between the tang and clevis to produce friction loads in the radial direction along the pins. An analysis of the model shows that such friction loads must be exceedingly high to prevent slippage and keep the tang tip from contacting the clevis. Therefore, slippage between the pins and the tang and clevis was assumed to occur which allows contact to take place between the tang tip and the clevis.

The outer lug displacements taken at several circumferential locations, are shown in the upper figure. The outer-lug displacement measured in the referee test by a typical displacement gage is shown in the lower graph. The test data exhibits the much steeper slope of the "friction, no contact line" up to 200 psi of pressure. Thus, it is concluded that friction forces on the pins prevent slippage up to 200 psi during the test and caused the much steeper initial slope for the displacement curve than indicated by the analytical results.

Above 200 psi pressure, the test data shows the rate of outer lug movement relative to the tang decreases, indicating contact taking place between the outer lug and the tang. Thus, extrapolating the test data at the higher pressures back to a zero pressure intercept gives an estimate of the outer lug initial clearance. The average of such extrapolated test data leads to the conclusion that the average outer lug clearance in the referee test is about 0.010 inch.

REFEREE TEST AND ANALYSIS CORRELATION

Effect of pin friction on outer lug motion



REFEREE TEST AND ANALYSIS CORRELATION

Effect of Pin Friction on Outer Lug Rotations

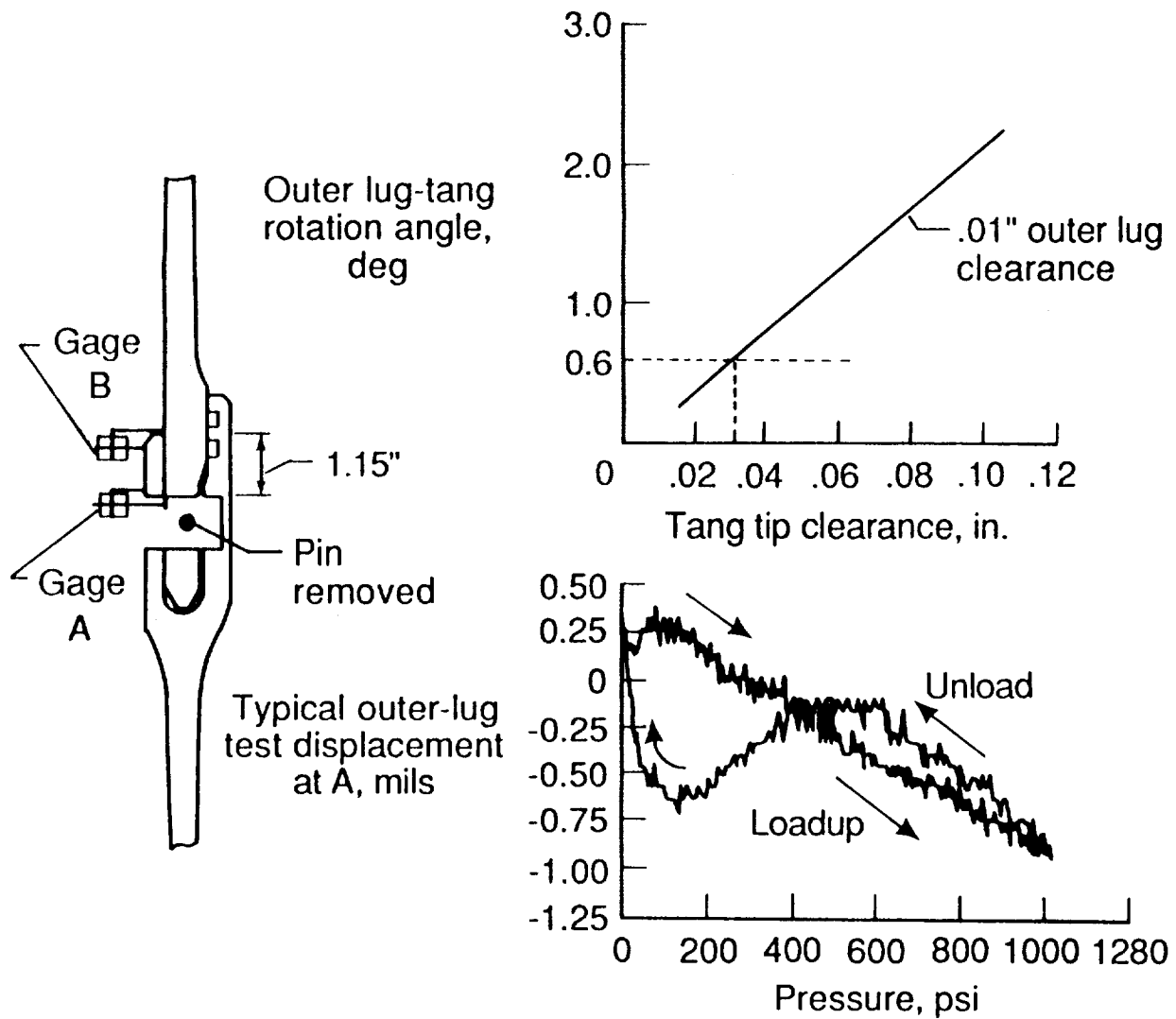
In the referee test, the relative displacements of the tang and outer lug were measured at the A and B gage locations shown in the sketch to the left of the figure. The A gage measured the relative radial displacement at the edge of the pinhole and thus required that the pin be removed during the test. The B gage, as discussed in the previous figure, measured displacement at the tip of the outer lug. Rotation of the outer lug relative to the tang is obtained by dividing the difference of the two gage readings, at any load level, by the 1.15 inch axial distance between the gages. The A and B gages, however, were not collocated at the same circumferential location. Therefore, the averages of the test data from gages A and B were used to find an average outer lug-tang rotation angle.

The displacement measured between the tang and outer lug by a typical gage at the edge of a pin hole at location A is shown in the figure. The A gage displacements are very small compared to the B gage displacement shown in the previous figure. In addition, the A test gage results change sign from one circumferential location to another. The average A gage displacement was -0.0003 or nearly zero. This confirms the analytical prediction that a point of zero relative displacement between the tang and outer lug occurs at the pin hole centerline. Large frictional forces between the tang and pins would also hinder displacements of the tang relative to the outer lug at the edge of the pin holes. The average B gage, or outer lug tip, displacement is 0.012 inch and is measured 1.15 inches away from location A. Therefore, the average relative rotation angle between the outer lug and tang is 0.6 degree. This is less than half the 1.5 degree rotation previously found possible within the nominal clearances in the joint.

The relative rotation angle between the outer lug and tang from the shell analysis is shown in the figure for various tip clearances. These results are for a 0.01 inch outer lug tip clearance. Changing the pin-induced moment from 2500 to 3000 in-lb/in gives no discernible difference in the plotted results, indicating that the rotation angle is not sensitive to the pin-induced moment acting on the inner lug. Intersecting the 0.6 degree relative rotation angle from test on the analytical curve indicates that the joint behaves as if it had an average tang tip clearance of about 0.03 inch. The previous referee test and analysis comparisons, however, do not support such a small tang tip clearance. The presence of friction forces on the pins influences the angle in much the same way as lug tip contact. Thus, it is concluded that friction causes the rotation data to indicate a tang tip clearance lower than actually exists.

REFEREE TEST AND ANALYSIS CORRELATION

Effect of pin friction on outer lug rotations



REFEREE TEST AND ANALYSIS CORRELATION

Tang Pull Out

The ends of the rocket motor case used for the referee test were closed, hence, the applied internal pressure created an axial tensile load in the shell wall. As pressure was applied, the axial load stretched the shell wall and pulled the tang and clevis joint in tension. Displacement gages, mounted at the position shown to the left of the figure, measured how much the tang pulled out from the clevis due to structural deformations. Eight of these gages were mounted around the circumference of the joint. The displacements measured at full pressurization from these eight gages were shown plotted in the upper part of the figure. Shown in the lower figure was the pull-out displacement measured by a typical pull-out displacement gage.

The initial pull-out displacement is a significant portion of the total pull-out displacement picked up by the gages. As the pressure was first applied, the the axial load pulled the tang out of the clevis to the extent allowed by the clearances between the pins and the pin holes. This initial pull-out displacement occurred at nearly zero pressure as evidenced in the figure by the sharp rise in the test displacement curve at nearly zero pressure. After the pin-hole clearance had been taken up the additional pull-out displacement was due to other mechanisms. Using a straight line extrapolation of the pull-out displacement curve back to intercept the zero pressure axis gave a good indication of the clearance around the pins. The average intercept value for the 8 gages gives an average clearance of 0.0035 inch (less than the 0.0085 inch single gage result shown in the lower figure).

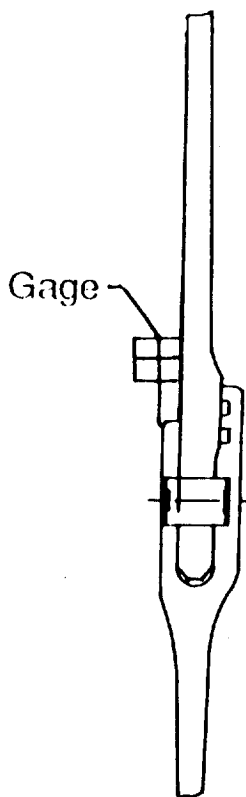
After the clearance around the pins has been taken up, bending and shearing deformation in the pins contribute to the tang pulling out from the clevis. These deformations, computed by handbook formulas assuming the pin to be a short beam under a 3 point load, was about 0.01 inch.

Elongations of the holes in the tang and in the clevis also contribute to the tang pulling out of the clevis. No simple formula for computing this elongation was found, but based on analytical strains in the shell wall around the holes, a rule of thumb of 0.5% of the hole diameter was adopted. Thus, the elongation of both the tang and clevis pin holes combine to give a pull out displacement of 0.01 inch. The contribution of the shell wall axial stretching to the pull out was found to be less than 0.001 inch.

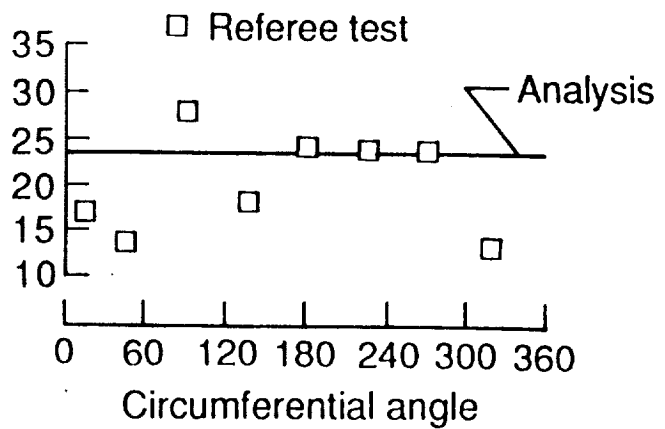
The average pin-hole clearance value plus the three analytical components of the pull out displacement summed up to be 0.024 inch. This result shown in the figure is in excellent agreement with the test results.

REFEREE TEST AND ANALYSIS CORRELATION

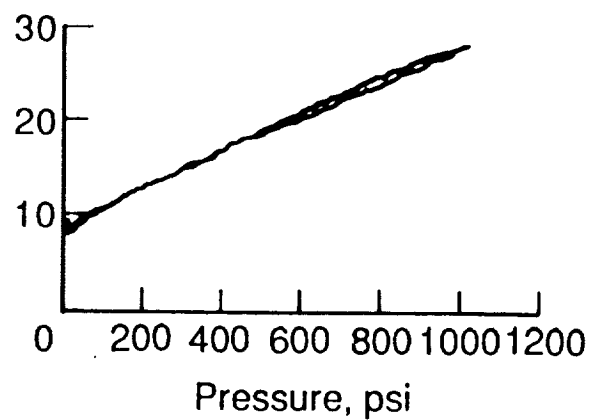
Tang pullout



Pullout displacement, mils



Typical pullout displacement, mils



REFEREE TEST AND ANALYSIS CORRELATION

Joint Strains

Strain gages were used in the referee test to measure the change in the girth of the rocket motor case as pressure was applied. The change in girth taken from the test gages was related analytically to the change in radius over radius. Therefore, analytical girth changes to compare with the test results were obtained by dividing radial displacements for the shell model by their corresponding shell radius. The shell model used to compute the analytical girth change had an outer lug clearance of 0.01 inch, a tang tip clearance of 0.046 inch and a pin-induced moment of 2000 in-lbs. The ratio of the test strain to the analytical strain was computed to facilitate comparing test and analysis results. Hence, perfect agreement between test and analysis would be indicated in the figure by a ratio of 1.0. The ratios of the test strains divided by the analytical strain values are shown in the figures for the various locations along the length of the shell.

As the results in the figure show, the agreement is excellent in the shell region away from the joint on the tang side, with the analytical strain agreeing within 5% of the test strain. On the clevis side, away from the joint, the agreement is poor because the shell model used for these results does not include the external ring stubs and wall thickness changes that are in the referee test hardware. Referring back to the previous analysis results that include the attach ring geometry, the computed radial displacement was 0.23 inch in the attach ring area. Using this radial displacement value for the clevis side of the joint gives a change in radius over radius value that agreed within 5% of the referee test results.

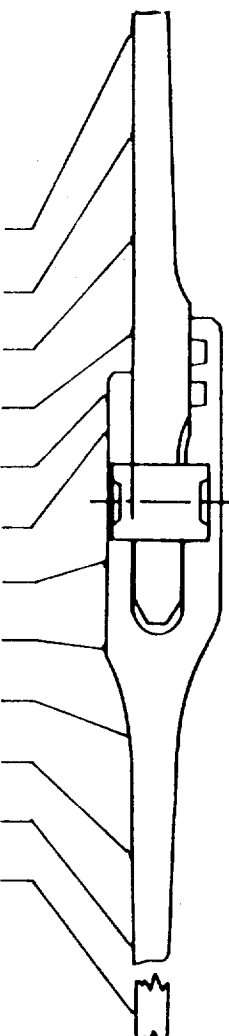
Within the joint, the test results are higher than the analysis indicating the analytical hoop stiffness is greater than the test hoop stiffness. Part of this higher hoop stiffness is due to the tapered thickness used for modeling the bolt holes. As discussed at the beginning of this study the thickness of the model at the pin hole centerline is chosen to match the bending stiffness across the pin-holes but the hoop stiffness is not matched. The result is a higher hoop stiffness in the model and lower analytical hoop strains within the joint as indicated in the figure.

Strains were computed for two other values of inner lug pin-induced moment, but their results showed that the girth strains are insensitive to the amount of pin-induced moment. Changes in tang tip clearance were made and these results showed this has a noticeable affect on the girth strain within the joint. Increasing the tang tip clearance by 0.01 inch to 0.056 inch, causes the girth strain ratios in the joint area to differ from test by as much as 31%. The ratios improve when a smaller tang tip clearance is used. However, the analysis results within the joint still differ from test by up to 20%.

REFEREE TEST AND ANALYSIS CORRELATION

Joint strains

Gage	Test (micro-inches)	Analysis (micro-inches)	=
1	(4200/4430)	= 0.95	
2	(3200/3072)	= 1.04	
3	(3100/2794)	= 1.11	
4	(3000/2570)	= 1.17	
5	(2750/2238)	= 1.23	
6	(2725/2246)	= 1.21	
7	(2700/2622)	= 1.03	
8	(2700/2621)	= 1.03	
9	(2800/2986)	= 0.94	
10	(2850/3225)	= 0.88	
11	(2725/3206)	= 0.85	
12	(3000/4265)	= 0.70	



CONCLUDING REMARKS

A study of the Shuttle 51-L SRB aft field joint was made using a shell-of-revolution analysis program. The study focused on mechanical features of the field joint and their influence on the O-rings during pressurization of the SRB case at launch ignition. The O-ring gap opening is defined as an increase in distance between the tang and the clevis inner lug midway between the two O-rings. The joint features studied include:

- 1) clearance between the clevis outer lug tip and the tang and contact between the outer lug tip and tang.
- 2) clearance between the tang tip and the clevis inner lug and contact between the tang tip and clevis.
- 3) distributed pressure on the inner lug.
- 4) eccentricity in application of the pin load at the clevis inner lug.
- 5) external stub rings aft of the field joint.

The study included correlation between analysis results and a hydro-static pressurization of a test SRB motor case. Based on results from the shell analysis the following conclusions are drawn:

1. The primary contributor to O-ring gap opening is tang/clevis contact and interaction within the joint. Without contact, relative rotations between tang and clevis alone are not significant contributors to the gap opening.
2. The second largest contributor to the gap opening is the moment induced by the pin reaction loads offset from the neutral axis of the inner lug.
3. A large clearance between the outer lug tip and the tang adversely affects the O-ring gap.
4. A small clearance between the tang tip and clevis inner lug adversely affects the O-ring gap.
5. Minor modifications to the structure of the joint are effective for causing the gap to close under pressurization.
6. Eliminating contact between the tang and clevis is a more efficient way of keeping the gap closed than eliminating rotations since schemes to eliminate rotations involve adding mass.

REFERENCES

1. Bushnell, David; Stress, Stability, and Vibration of Complex Branched Shells of Revolution: Analysis and Users' Manual for BOSOR4. NASA CR-2116, Oct. 1972.
2. SRM Joint Deflection Referee Test: Phase II Final Report. Morton Thiokol Inc., TWR-300149, April 3, 1986.



Report Documentation Page

1. Report No. NASA TM-102748	2. Government Accession No.	3. Recipient's Catalog No.	
4. Title and Subtitle A Parametric Shell Analysis of the Shuttle 51-L SRB AFT Field Joint		5. Report Date October 1990	
		6. Performing Organization Code	
7. Author(s) Randall C. Davis, Lynn M. Bowman, Robert M. Hughes IV, and Brian J. Jackson		8. Performing Organization Report No.	
		10. Work Unit No. 506-43-71-04	
9. Performing Organization Name and Address NASA Langley Research Center Hampton, VA 23665-5225		11. Contract or Grant No.	
		13. Type of Report and Period Covered Technical Memorandum	
12. Sponsoring Agency Name and Address National Aeronautics and Space Administration Washington, DC 20546-0001		14. Sponsoring Agency Code	
15. Supplementary Notes R. C. Davis - Langley Research Center, Hampton, Virginia. L. M. Bowman - Lockheed Engineering and Sciences Company, Hampton, Virginia. R. M. Hughes IV and B. J. Jackson - Old Dominion University, Norfolk, Virginia			
16. Abstract The shell-of-revolution computer program BOSOR4 is used to model and analyze the aft field joint of the Shuttle 51-L solid rocket booster (SRB) motor. The shell model incorporates the SRB wall and joint geometry present during the Shuttle 51-L flight. A series of analyses is made that determines what effects various structural features in the joint have on the O-ring seals in the joint. The structural features considered include joint clearances, contact between the joint components, pin induced loads, pressure distributions, and geometric nonlinearity. Also, various proposed modifications to the joint are analyzed. Finally, analytical results are compared with results from a hydro-static test of an SRB case with a joint.			
17. Key Words (Suggested by Author(s)) SRB Field Joint, Shell Analysis Shell Contact, Clearance Effects, Test Comparison, Solid Rocket Booster Case, and Shuttle Test Comparison		18. Distribution Statement Unclassified - Unlimited Subject Category - 39	
19. Security Classif. (of this report) Unclassified	20. Security Classif. (of this page) Unclassified	21. No. of pages 48	22. Price A03